HHS Public Access

Author manuscript

J Control Release. Author manuscript; available in PMC 2020 June 10.

Published in final edited form as:

J Control Release. 2019 June 10; 303: 109–116. doi:10.1016/j.jconrel.2019.04.013.

Prevention of Paclitaxel-Induced Neuropathy by Formulation Approach

Xiaowei Zang, **Jong Bong Lee**, **Kiran S. Deshpande**, **Olga B. Garbuzenko**, **Tamara Minko**, **Leonid Kagan**

Department of Pharmaceutics, Ernest Mario School of Pharmacy, Rutgers, The State University of New Jersey, Piscataway, NJ

Abstract

Chemotherapy-induced peripheral neuropathy (CIPN) is a major adverse effect of paclitaxel. Several liposome-based products have been approved and demonstrated superior efficacy and safety profiles for other drugs. The first objective of this work was to evaluate the effect of liposome formulation of paclitaxel (L-PTX) on neurotoxicity *in-vitro* and *in-vivo* in comparison to the standard Taxol® formulation. The second aim was to investigate the effect of formulation on paclitaxel biodistribution following intravenous administration in an animal model. Free paclitaxel was toxic to cell of neuronal origin (IC50 = 18.4 μg/mL) at a lower concentration than to lung cancer cells (IC50 = 59.1 μg/mL), and L-PTX demonstrated a comparable toxicity to both cell lines (IC50 = 31.8 and 33.7 μg/mL). Administration of L-PTX at 2 mg/kg per dose for a total of 4 doses on day 0, 2, 4, and 6 to rats did not result in increased sensitivity in response to mechanical or thermal stimulation of hind paws, in comparison to Taxol® administration at the same dose level that resulted in neuropathy. Paclitaxel biodisposition was evaluated for two formulations in plasma, liver, lung, brain, spinal cord, skin and muscle of rats after single intravenous dose at 6 mg/kg. The exposure to paclitaxel in brain, spinal cord, muscle, and skin was lower in the L-PTX group compared to Taxol® group. PEGylated liposomes containing paclitaxel were successfully developed and demonstrated reduced neurotoxicity *in-vitro* in neuronal cells and prevented development of peripheral neuropathy *in-vivo*. Proof of concept study was performed and showed that formulation in nanoparticles is a promising approach for reducing (or preventing) neurotoxicity caused by cancer drugs.

Keywords

paclitaxel; chemotherapy-induced peripheral neuropathy; liposomes; formulation; biodistribution; neurotoxicity; nanoparticles

Corresponding author: Leonid Kagan, Ph.D., Department of Pharmaceutics, Ernest Mario School of Pharmacy, Rutgers, The State University of New Jersey, 160 Frelinghuysen Road, Piscataway, NJ 08854, Tel: (848) 445-6365, Fax: (732) 445-3134, lkagan@pharmacy.rutgers.edu.

INTRODUCTION

In 2014, it was estimated that more than 14.5 million cancer survivors were living in the US, and this number was estimated to increase to 19 million by 2024 (2). Based on recent data from the Center of Disease Control and Prevention, about 650,000 cancer patients receive chemotherapy in an outpatient oncology clinic in the US. Highly effective treatments have been developed, and the increase in survival demands more attention to patients' quality of life and management of adverse effects.

Chemotherapy-induced peripheral neuropathy (CIPN) is a major, often dose-limiting adverse effect of various cancer therapies (3). Taxanes (paclitaxel, docetaxel) is one of the six main classes of agents that induce toxicity to peripheral sensory and motor neurons that leads to CIPN. Other drugs associated with CIPN include platinum-based chemotherapeutics (cisplatin, carboplatin, oxaliplatin), proteasome inhibitor (bortezomib), immunomodulator (thalidomide), epothilones (ixabepilone), and vinca alkaloid (vincristine and vinblastine). Up to 40–90% of patients treated with neurotoxic chemotherapy will develop CIPN, which may lead to long-term morbidity and reduced quality of life. CIPN can be particularly severe and long-lasting (4), symptoms have been reported for up to 11 years after completion of therapy (5). Neuropathic pain is one of the most challenging pain conditions with poor response to pharmacotherapy (6); therefore, discontinuation of chemotherapy or dose reduction often remain the only clinical solution (7).

Paclitaxel is used for treatment of various cancers, including ovarian, breast, small and non-small-cell lung, colon, bladder, esophagus, head and neck, multiple myeloma, and advanced forms of Kaposi's sarcoma (8, 9). It was the first in a new class of microtubule stabilizing drugs that inhibit mitosis and normal cell division by stimulating the polymerization of tubulin (10–13). Paclitaxel is a Biopharmaceutics Classification System class IV drug with high lipophilicity (logP~4) and poor aqueous solubility (0.77 – 35 μM) (14–17). Taxol® (the first approved formulation of paclitaxel by Bristol-Myers Squibb Company) is formulated with polyoxyethylated castor oil (Cremophor EL) and ethanol (1:1, v/v) due to the poor solubility of the drug. Although highly efficacious, several severe (and often dose-limiting) adverse events were reported with Taxol® treatment, including peripheral neurotoxicity (42–70%), nephrotoxicity (18–34%) and hypersensitivity (31–45%) (reported as percentages of patients after single-agent therapy) (18). Presence of Cremophor EL in the formulation was reported to contribute to mechanical hyperalgesia after five weekly intravenous (IV) doses in rodents (19), and it is a major cause of hypersensitivity reactions. While some other formulations of paclitaxel became available, Taxol® remains the standard of care for many cancers.

For successful clinical use, efficacy of a drug should be balanced with an acceptable level of adverse reactions. Several liposome-based products have been approved and demonstrated superior efficacy and safety profiles. For example, Doxil® (PEGylated liposomal doxorubicin) that is used for Kaposi's sarcoma and recurrent ovarian cancer enhanced the bioavailability at the tumor site and reduced side effects (20–22). AmBisome® (liposomal amphotericin B) significantly improved toxicity profile compared to conventional amphotericin B while retaining the antifungal effect (23). Although multiple groups

developed various particulate formulations of paclitaxel, the majority of efforts was focused on enhancing delivery to the tumor and improving efficacy. Reducing toxicity, and especially neurotoxicity, of these formulations was not a primary objective and was rarely tested. Only one liposomal paclitaxel formulation, Lipusu®, was approved for clinical use by the Chinese Food and Drug Administration (24); and liposomal paclitaxel formulation is not available in the US yet.

The first aim of this work was to evaluate the effect of liposome formulation of paclitaxel (L-PTX) on neurotoxicity in comparison to the standard Taxol® formulation. The second aim was to investigate the effect of formulation on paclitaxel biodistribution following IV administration in a preclinical model.

MATERIALS AND METHODS

Materials

Taxol® (6 mg/mL, Teva, North Wales, PA) was generously provided by Rutgers Cancer Institute of New Jersey (New Brunswick, NJ). Paclitaxel was purchased from Sigma Aldrich (St. Louis, MO). A549 human non-small-cell lung adenocarcionoma epithelial cells were purchased from American Type Culture Collection (ATCC, Manassas, VA) and human neuroblastoma SH-SY5Y cells were generously provided by Dr. Kiledjian's laboratory at Rutgers University. Egg phosphatidylcholine (egg PC), cholesterol, and 1,2-distearoyl-*sn*-glycero-3-phosphoethanolamine-N-[methoxy(polyethylene glycol)-2000] (ammonium salt) (mPEG 2000) were purchased from Avanti Polar Lipids (Alabaster, AL). All other chemicals were of analytical grade, and solvents were of HPLC grade.

Synthesis and Characterization of Liposomes Containing Paclitaxel

Drug-loaded liposomes were prepared with three lipids as described previously (25). Briefly, PEGylated liposomes were formulated from egg PC:cholesterol:mPEG 2000 in mole ratio 55:40:5 by dissolving in 100% ethanol and loading with paclitaxel. The solution was subsequently evaporated to a thin film layer using a rotary evaporator Rotavapor® R-210/R-215 (BUCHI Corp., New Castle, DE) and rehydrated with 0.9% NaCl to final lipid concentration 20 mM. The suspension was aliquoted to 5 mL in a small glass vial for probe sonication to obtain a more homogenous population of nanosized liposomes (Fisher Scientific Model 120 Sonic, Waltham, MA, 50 constant output for 4 min with 15 sec/cycle and 5 sec pauses to avoid overheating). The probe was immersed to a depth of 15 mm above the bottom of the glass vial. The time for sonication was optimized to obtain a mean diameter of 50–60 nm. Free paclitaxel was separated from liposomes by dialysis using dialysis membrane with pore size 50 kDa (Spectrum Labs, New Brunswick, NJ) against 100 volumes of 0.9% NaCl three times (0.5 h, 3 h, and overnight) at 4°C.

The particle size distribution was measured by Malvern ZetaSizer NanoSeries (Malvern Instruments Enigma Business Park, UK) according to the manufacturer's instruction. All measurements were carried out at room temperature. The stability of liposome was monitored up to 4 weeks at 4 °C. The free drug was removed by dialysis as described above. Encapsulation efficiency of paclitaxel was determined (after free drug was separated from

the liposomes) using the following formula, $Percent\ encapsulated = \frac{[Total\ paclitaxel] - [Free\ paclitaxel]}{[Total\ paclitaxel]} \times 100\%$. The concentration of paclitaxel encapsulated in liposomes was further determined by the HPLC. Each parameter was measured three times for each batch, and average and standard deviations were calculated.

Cell Culture and Cell Viability Study

The experiments were carried out using two cell lines. A549 human lung carcinoma cells were cultured in RPMI 1640 medium (Corning, Manassas, VA) supplemented with 10% fetal bovine serum (Corning, Manassas, VA). SH-SY5Y human neuroblastoma cells were cultured in Dulbecco's modified Eagle's medium / Ham's F-12 50/50 mix (Corning, Manassa, VA) supplemented with 10% fetal bovine serum. Both cell lines were maintained in tissue culture-treated dish (Falcon, Catalog No. 353003, Durham, NC). All cells were grown at 37°C in a humidified atmosphere of 5% CO_2 (v/v) in air and passed every 3–4 days. The experiments were performed on cells in the exponential growth phase.

Cell viability was assessed using CellTiter-Fluor™ assays (Promega Corporation, Madison, WI) that was performed according to the manufacture's protocol. Briefly, 50,000 cells/well of SH-SY5Y cells and 20,000 cells/well of A549 cells were plated in the 96-well plate with the complete medium. After 24 hours, the cells were treated with either paclitaxel or liposomal paclitaxel at 0.1, 0.2, 0.39, 0.78, 1.56, 3.13, 6.25, 12.5, 25, 50, 100 μg/mL for another 24 h with 0.1% DMSO in all wells. On the third day, cell viability was assessed by CellTiter-Fluor™ assay using a microplate reader Spectra Max M3 (Molecular Devices, San Jose, CA) with excitation and emission wavelengths of 390 and 505 nm. Untreated cells (medium only) served as a negative control (100% viability), and cells treated with 0.1% Triton X-100 in medium served as a positive control for maximal cytotoxicity. Cell viability tests were performed in triplicate.

In-Vivo Neurotoxicity Study

Veterinary care followed the guidelines of the Association for Assessment and Accreditation of Laboratory Animal Care (AAALAC), and all procedures were approved by the Rutgers Institutional Animal Care and Use Committee (IACUC). Adult (140–160 g) male Sprague-Dawley rats (Envigo, Somerset, NJ) were used for all experiments. Rats were housed two per cage in a temperature- and humidity-controlled room on a 12:12 h light:dark cycle with free access to food (Catalog No. 5001, LabDiet, St. Louis, MO) and water. All experiments were performed during the same period of the day (8:30 am to 12:00 pm) to avoid diurnal variations in animal responses.

The animal study was conducted to evaluate the difference in paclitaxel-induced peripheral neuropathy in rats following administration of L-PTX and the control formulation (Taxol®). A previously reported *in-vivo* model of Taxol®-induce peripheral neurotoxicity (increased sensitivity of hind paws to mechanical and thermal stimuli) was used (26). In this model, development of neurotoxicity is observed after a few days following a series of IV injections of Taxol® with animal recovery after approximately 4–5 weeks.

Baseline sensitivity of animals to mechanical and thermal stimuli was measured for 3–4 times before drug administration (as described below). The investigator collecting behavioral data was blinded to the treatment group assignment. Rats were randomly assigned to two treatment groups (n=10 each). Neuropathy was induced by repeated IV dosing of paclitaxel at a cumulative dose of 8 mg/kg (2 mg/kg, every other day for a total of 4 doses) (26, 27). Prior to administration, Taxol® was freshly diluted in sterile normal saline and injected at a concentration of 1 mg/mL. Liposomal paclitaxel (L-PTX) formulation was freshly prepared two days before injection at a concentration of 1 mg/mL. Rats were administered dosing solutions via the tail vein (under isoflurane anesthesia) on days 0, 2, 4, and 6. Drug administration was performed after animal sensitivity thresholds were measured.

Assessment of sensitivity of rats to mechanical stimuli was performed using the dynamic plantar aesthesiometer (Ugo Basile, Italy), as previously described (28). Rats were habituated to the testing procedure, equipment, and the investigator for two or three days before the collection of baseline data. To obtain a reliable baseline, rats' sensitivity was measured on at least 3 consecutive days. Briefly, rats were left to habituate inside plastic enclosures on top of a perforated platform before starting the measurement for approximately 30 min. A linearly increasing force was applied on the plantar surface of hind paws using a metal filament which was programmed with the microprocessor (2.5 g/s, with a cut-off of 50g). A "positive response" signal was automatically recorded when the animal withdrew the paw. Withdrawal thresholds in response to the mechanical stimuli was recorded in grams. Each animal was tested 3 times with a 5-min interval, and the average of the 3 measurements for each paw was considered the withdrawal threshold.

Assessment of sensitivity of rats to thermal stimuli was performed using the Hargreaves apparatus (plantar test) (Ugo Basile, Italy), as previously described (29). Similar to the assessment of mechanical sensitivity, rats were habituated before the study and a reliable baseline was established before drug administration. Briefly, rats were left to habituate inside plastic enclosures on top of a glass surface for approximately 30 min. A radiant heat source was located below the glass platform. The paw withdrawal reaction time of rats exposed to a radiant heat on their plantar surface of hind paws was recorded with a precision margin of 0.1 s. The response of the animal was calculated by taking the average of 3 measurements with a 5-min interval. The maximum time was set to 20 s to prevent damage to the plantar surfaces.

Paclitaxel Tissue Disposition Study

Sprague-Dawley rats were used to investigate the effect of formulation on the biodistribution of paclitaxel after IV administration. Rats were randomly divided to receive a single dose of 6 mg/kg of Taxol® or L-PTX via the tail vein. Animals were sacrificed under isoflurane anesthesia (n=3–4 for each time point). Blood and tissue (liver, lung, brain, spinal cord, skin, and muscle) samples were collected at 0.5, 1, 2, 4, and 6 h after drug injection. Blood samples were collected into heparinized tubes and immediately processed for plasma by centrifugation at 1300 × g for 10 min. Tissue samples were washed with saline and blotted dry with Kimwipes to remove excess fluid. Samples were stored at −80°C until analysis.

Bioanalytical procedure

The analysis of paclitaxel was carried out using an HPLC-UV system (Agilent 1260 Infinity, Santa Clara, USA). A reverse phase column EC-C18 (4.6 × 100 mm, 2.7 μm) (Agilent, Santa Clara, USA) was used at 45 °C. The mobile phase consisted of a mixture of (A) acetonitrile and (B) water with the following gradient scheme: 0 – 1 min, A – 30%; 1 – 8 min, A increased to 85%; 8 – 8.5 min, A – 85%; 8.5 – 8.7 min, A decreased to 30%; 8.7 – 10 min, A – 30%. The run time was 10 min with flow rate of 1.0 mL/min. The detector wavelength was set at 225 nm. Retention times for paclitaxel and internal standard (N-benzylbenzamide) were 7.0 and 5.0 min. The lower limit of quantification for paclitaxel was 50 ng/mL, and the method was linear between 50 and 20,000 ng/mL.

Paclitaxel was extracted from plasma samples using a liquid-liquid extraction method. Briefly, 100 μL of plasma was mixed with 10 μL of N-benzylbenzamide (100 μg/mL in acetonitrile, internal standard), 300 μL of acetonitrile, and 3 mL of methyl tert-butyl ether by vortexing for 10 min and followed by centrifugation for 5 min at 3000 rpm. The supernatant was transferred to new glass tubes and evaporated under a light stream of nitrogen at 40°C. The residue was reconstituted with 100 μL of 50% acetonitrile in water and filtered through a 0.2 μM nylon filter (Thermo scientific, Rockwood, TN). The injection volume was 40 μL.

Liver, lungs, brain, and spinal cord were sliced into strips and weighted. The density of all tissues was assumed to be 1 mg/mL. Each tissue was mixed with PBS (a double volume of the sample) and 0.5 mm zirconium oxide beads or 3.2 mm stainless steel round beads followed by 3–4 min of homogenization at speed 8, 12, or 20 (Bullet Gold Blender®, Next Advance, Troy, NY). Skin and muscle were sliced into strips and mixed with PBS (a quadruple volume of the sample) followed by homogenization. Paclitaxel was extracted from tissue homogenates using a solid phase extraction method. Briefly, tissue homogenate (100 μL for liver, lungs, brain, and spinal cord or 200 μL for skin and muscle) were combined with an equal amount of methanol and the internal standard (10 or 20 μL, respectively). The samples were then vortexed for 20 s and centrifuged at 13,000 rpm for 5 min. The supernatant was transferred to the preconditioned cartridges (Bond Elut Plexa 30mg, Agilent, Santa Clara, CA) followed by washing with 5% methanol in water, then eluted by applying 400 μL of methanol twice. The eluent was evaporated and reconstituted as described for plasma extraction. For each tissue a separate calibration curve was used using the corresponding blank tissue matrix.

Data Analysis

Mean plasma and tissue concentrations of paclitaxel at each time point were calculated for both formulations. Noncompartmental analysis was completed using a Phoenix WinNonlin version 7.0 (Pharsight Corp., California, USA). Logarithmic trapezoidal method was used to calculate the area under the concentration-time curve to the last available timepoint (AUC_{last}).

Data from different experiments are presented as mean ± SD. For statistical analysis of the differences in mechanical and thermal sensitivity between two administration groups, Student’s t-test of independent means was used. A value of $P < 0.05$ was considered

statistically significant. Cell viability analysis and determination of IC50 values were conducted using GraphPad Prism 7 software.

RESULTS

Liposomal formulation of paclitaxel was developed and characterized. The size of the liposomes containing paclitaxel was 140 ± 13 nm, and the encapsulation efficiency was 99.6% ± 3.6%. The liposomes had a slight negative charge (−6.78 ± 1.32 mV). The formulation stability in the 4 °C was evaluated for up to 4 weeks. After a week of storage in the 4 °C, 79% of the drug was encapsulated in the liposome after a second round of dialysis; the particle size did not change. After 4 weeks, 67% of the drug was encapsulated in the liposomes after dialysis, the particle size slightly increased to 156 ± 12 nm.

The cytotoxicity of L-PTX formulation was compared with paclitaxel with human lung carcinoma A549 (Figure 1a) and human neuroblastoma SH-SY5Y (Figure 1b) cell lines. The IC50 value for A549 cells for paclitaxel solution and L-PTX were 59.1 and 33.7 μg/mL. The IC50 value for SH-SY5Y cells for paclitaxel solution and L-PTX were 18.4 and 31.8 μg/mL. The study showed that free paclitaxel was toxic to cell of neuronal origin at a lower concentration than to lung cancer cells, and liposomal formulation demonstrated a comparable toxicity to both cell lines. In addition, empty liposomes at several dilutions (corresponding to the dilutions of L-PTX) did not affect the viability of cell cultures.

To evaluate the effect of pharmaceutical formulation on paclitaxel-induced neurotoxicity, changes in rat sensitivity to mechanical and thermal stimulation of hind paws was tested after administration of Taxol® and L-PTX formulations by IV route at 2 mg/kg per dose for a total of 4 doses on day 0, 2, 4, and 6 (Figure 2a). The study was initiated when the animals were at 6 weeks of age. The baseline response to mechanical stimulation before drug administration was similar between the groups (30.17 ± 1.15 g for Taxol®, and 29.62 ± 0.77 g for L-PTX). Administration of Taxol® resulted in a significant reduction of withdrawal threshold in response to mechanical stimuli from day 9 to day 26 after the first drug injection (as compared to the baseline threshold). In comparison, administration of L-PTX did not result in increased sensitivity to mechanical stimulation. From day 4 till day 34, a statistically significant difference was observed between the groups. The nadir of reduction (24.64 ± 2.17 g) for Taxol® treated rats was achieved on day 11 as compared to the measurement of 38.04 ± 3.55g for L-PTX treated rats on the same day.

Animals in both groups returned to a similar withdrawal threshold after day 36, at which time Taxol® group had a withdrawal threshold of 40.11 ± 4.82 g compared to 40.71 ± 5.32 g for L-PTX treated rats. The withdrawal threshold by the end of the study was higher than the baseline before paclitaxel injections. An increase in withdrawal threshold with age (and body weight) was previously observed in a separate animal cohort without paclitaxel administration (Figure 2b), from 30.2 ± 3.6 g on week 6 to 45.4 ± 2.0 g on week 10.

In addition, animal sensitivity to thermal stimuli was investigated in animals receiving Taxol® or L-PTX formulations at 2 mg/kg every other day for a total of 4 doses (Figure 3). The baseline sensitivity before drug administration was similar between two groups, 12.99

± 2.48 s for Taxol® and 14.32 ± 3.60 s for L-PTX treated group. Taxol® treatment produced a significant reduction in reaction time to heat stimulation, from day 9 to day 26 after the first drug dose administration compared to the L-PTX treatment group. The nadir of reduction of the response time was on day 18, when Taxol®-treated rats had a reaction time of 10.80 ± 1.61 s compared to 17.87 ± 3.00 s for L-PTX-treated rats. For technical reasons thermal thresholds were not measured beyond day 26.

To investigate the effect of formulation of paclitaxel biodisposition, Sprague-Dawley rats were given a single IV injection of Taxol® or L-PTX at 6 mg/kg dose level. The time-course of drug concentrations in the plasma and tissues was determined (Figure 4 and Table 1). The disappearance of paclitaxel from plasma was faster for L-PTX than for Taxol® group. Plasma concentration extrapolated to time zero (C_0) and the area under the plasma concentration-time curve (AUC to the last measured concentration) for Taxol® group were 3.5-fold and 6.2-fold higher than for L-PTX, respectively. Furthermore, plasma half-life of paclitaxel was 3.2 times longer for Taxol® than for L-PTX group.

Biodistribution of paclitaxel to liver and lungs was studied because the reticuloendothelial system represents a major mechanism for clearance of circulating liposomes. L-PTX was taken up by the liver to a greater extent than was Taxol®; the concentration of paclitaxel at 0.5 h was 112.7 ± 11.4 μg/mL for L-PTX and 30.6 ± 2.7 μg/mL for Taxol®. In the lungs, the drug concentration at 0.5 h was 46.2 ± 7.7 μg/mL for L-PTX and 12.2 ± 1.2 μg/mL for Taxol®. As neurotoxicity was the main focus of the study, exposure to paclitaxel in the nervous system (brain and spinal cord) and in the skin and muscle (location of sensory axons) was evaluated. The exposure to paclitaxel in the skin, muscle, brain, and spinal cord was lower in the L-PTX group compared to Taxol® group. In the brain and spinal cord, the concentration of paclitaxel at 0.5 h was 138.0 ± 26.1 ng/mL and 111.8 ± 20.4 ng/mL for L-PTX group; and 220.6 ± 34.3 ng/mL and 134.1 ± 28.5 ng/mL for Taxol® group. In the skin and muscle, the concentration of paclitaxel at 0.5 h was 462.9 ± 187.3 ng/mL and 289.3 ± 87.3 ng/mL for L-PTX group; and 1973.9 ± 373.2 ng/mL and 2236.5 ± 460.2 ng/mL for Taxol® group. Drug concentration for plasma, brain and spinal cord after 2 h time points was below the lower limit of quantification.

To further highlight the difference between paclitaxel exposure between two formulations, the ratio of paclitaxel concentrations in various tissues between Taxol®- and L-PTX-treated groups was calculated (Figure 5).

DISCUSSION

Chemotherapy-induced neuropathy is a very common, serious, and debilitating adverse effect of paclitaxel and many other anticancer drugs. Common neuropathic symptoms include numbness, tingling, pain or impaired sensory function in hands and/or feet, hypersensitivity to mechanical and cold stimuli, clumsiness in fingers, peripheral muscular weakness or difficulties in walking (30). CIPN is often presents in a “stocking and glove” pattern in feet and hands because longer axons are affected first (31). Variable statistics exists regarding the prevalence of CIPN, depending on the study design and assessment period. A recent systematic review (31 studies, 4179 patients) reported CIPN prevalence of

68% when measured in the first month after chemotherapy, 60% at 3 months and 30% at 6 months or more (32). Prevalence as high as 80–90% has been reported (33, 34). Different drugs may result in a different clinical presentation of neuropathy symptoms; the underlying mechanism of development of CIPN are complex (34, 35) and not fully understood. The pathophysiological changes caused by paclitaxel include immune-mediated processes, loss of peripheral fibers, demyelination and axon degradation, and mitochondrial dysfunction (36). Treatment of CIPN is mostly symptomatic (using anticonvulsants, gabapentin, opioids (7)) and remains largely ineffective (6). Some prevention treatments using vitamin E, amifostine, and glutathione were reported (7); however, discontinuation of chemotherapy or dose reduction remains the only clinical solution (7). Therefore, there is an urgent need to develop approaches for prevention of CIPN.

Taxol® remains the standard therapy for many cancers, although some other formulations are available. Abraxane®, a nanoparticle albumin-bound paclitaxel formulation (Cremophor EL-free), was approved in the US in 2005. However, this formulation also resulted in dose-dependent mechanical and cold allodynia in rats, which tended to be even stronger (in degree of sensitivity) than that of Taxol® at the doses used clinically (37). Later, polymeric micelle (Genexol®-PM) and liposome formulations (Lipusu®) of paclitaxel were approved in Korea and China, respectively. The incidence for peripheral neurotoxicity did not differ significantly between Genexol®-PM and Taxol® treatments in recurrent or metastatic HER2negative breast cancer patients (38). Limited information could be found for Lipusu® treatment, and the incidence of peripheral neurotoxicity was reported as 62% in the package insert (39).

Preclinical formulation development for paclitaxel and other cancer drugs is often primarily focused on tumor targeting and overall efficacy, without specifically considering adverse effects and especially neurotoxicity. Only two groups reported assessment of neurotoxicity as a part of formulation development for paclitaxel. A phase I study with a polymerconjugated prodrug of paclitaxel in refractory solid tumors patients was discontinued prematurely because of severe neurotoxicity - 4 out of 12 patients developed grade 2–3 peripheral neuropathy (40). Another micellar nanoparticle formulation was found to be less neurotoxic than free paclitaxel; however, only *in-vitro* studies were completed (41).

In this study, the liposomal formulation of paclitaxel was less toxic to neuronal cells than paclitaxel solution and prevented development of neurotoxicity *in-vivo* as compared to Taxol® administration (that resulted in a significant increase in sensitivity of rats to mechanical and thermal stimuli). In the animal study, rats were randomly assigned to treatment groups and the investigator that measured sensitivity thresholds was blinded to the treatment group assignment. Moreover, the results closely resembled our pilot study with 5 animals in each group (L-PTX vs. Taxol®, data not shown). The time-course of dynamics of animal responses (increased sensitivity followed by a recovery phase) after administration of Taxol® in our study was also similar to previous result by other investigators (26). Increased sensitivity to mechanical stimuli developed on day 4 after first injection of Taxol®, and animals recovered on day 37.

In this study, L-PTX showed lower IC50 in lung cancer cells compared to paclitaxel solution. We have previously showed that nontargeted and targeted liposomal formulations of paclitaxel are effective in suppression of tumor growth in nude mice bearing human A549 lung carcinoma xenografts (25). Future studies in orthotopic cancer mice models are needed to simultaneously assess efficacy and toxicity and establish dose-response relationships tor L-PTX. High paclitaxel exposure in the lungs following administration of L-PTX further supports potential use of this formulation for lung cancer.

Assessment of drug concentration in target tissues is important for establishing dose-response relationships for efficacy and toxicity. Previously, we developed a physiologically-based pharmacokinetic (PBPK) model to describe paclitaxel biodistribution after Taxol® administration based on published data (1). In this type of mathematical models, the body is represented by a series of physiological compartments corresponding to various organs and connected by perfusing blood; and model parameters were estimated to characterize whole-body disposition of paclitaxel. The model was developed based on rodent data and successfully predicted paclitaxel concentration-time profiles in humans after administration of Taxol. Extensive variability in reported tissue concentrations was found across multiple publications. Some of the differences were attributed to bioanalytical procedures and other experimental techniques. Observed tissue concentration data of paclitaxel after Taxol® dosing obtained in this study were in good agreement with model-based predictions generated based on our previously developed PBPK model, which further qualifies the model (Figure 6) (1).

In majority of previous studies paclitaxel disposition to the brain and other parts of the nervous system was not reported. Furthermore, assessment of drug disposition into skin and muscle is rarely evaluated, and these tissues are lumped in a “remainder” compartment in PBPK models. In this study, we evaluated concentrations of paclitaxel in tissues that may help establish dose-CIPN relationships, including peripheral tissues (skin and muscle) where sensory axons are located (7) and the central nervous system (spinal cord and brain). Changes in the CNS due to administration of paclitaxel have been previously reported, e.g. increased reactive nitrogen species production in the spinal cord of rats (42) and increased expression of voltage gated sodium channel in forebrain of mice (43). Persistent muscle and cutaneous hyperalgesia were observed in Taxol® induced peripheral neuropathy in rats (44). Administration of L-PTX led to a significantly lower drug exposure in the brain, spinal cord, muscle and skin compare to Taxol®-treated group, which corresponds to the results of mechanical and thermal sensitivity testing.

Surprisingly low concentrations of paclitaxel in the plasma and short circulation half-life were obtained after L-PTX dosing, which may be related to efficient uptake by the reticuloendothelial system. The size of the particles was relatively small for liposomes with mPEG 2000, which might be caused by probe sonication during formulation preparation. Future studies are needed to determine the optimal size of particulates for preserving (or enhancing) efficacy and minimizing neurotoxicity. In a previous animal study, no correlation was found between Taxol® dose (0.5–2 mg/kg) and the extent of neuropathy (27). However, the exposure of the nervous system to paclitaxel was not tested. Dose-response relationships

for L-PTX will be addressed in future studies that will require more sensitive bioanalytical methods.

CONCLUSION

Proof of concept study was performed and showed that formulation in nanoparticles is a promising approach for reducing (or preventing) neurotoxicity caused by cancer drugs. L-PTX significantly reduced cytotoxicity *in-vitro* in neuronal cells and prevented development of peripheral neuropathy *in-vivo.* Future studies with simultaneous assessment of anticancer efficacy and neurotoxicity in tumor-bearing animals are needed for development of an optimized formulation for paclitaxel; and this approach can be potentially extended to other neurotoxic compounds.

ACKNOLEDGMENT

This work was supported in part by the R01 grants (CA209818 and GM124046) from the National Institute of Health. The authors would like to thank Dr. Andriy Kuzmov for his generous help with formulation development.

ABBREVIATIONS

CIPN	chemotherapy-induced peripheral neuropathy
IV	intravenous
L-PTX	liposomal paclitaxel

REFERENCE

1. Zang X, Kagan L. Physiologically-based modeling and interspecies prediction of paclitaxel pharmacokinetics. J Pharmacokinet Pharmacodyn. 2018. doi: 10.1007/s10928-018-9586-9.
2. DeSantis CE, Lin CC, Mariotto AB, Siegel RL, Stein KD, Kramer JL, Alteri R, Robbins AS, Jemal A. Cancer treatment and survivorship statistics, 2014. CA Cancer J Clin. 2014;64(4):252–71. doi: 10.3322/caac.21235. [PubMed: 24890451]
3. Farquhar-Smith P, Brown MRD. Persistent Pain in Cancer Survivors: Pathogenesis and Treatment Options. Pain Clinical Updates XXIV. 2016;4:1–8.
4. Cavaletti G, Alberti P, Marmiroli P. Chemotherapy-induced peripheral neurotoxicity in cancer survivors: an underdiagnosed clinical entity? Am Soc Clin Oncol Educ Book. 2015:e553–60. doi: 10.14694/EdBook_AM.2015.35.e553.
5. Beijers AJ, Mols F, Tjan-Heijnen VC, Faber CG, van de Poll-Franse LV, Vreugdenhil G. Peripheral neuropathy in colorectal cancer survivors: the influence of oxaliplatin administration. Results from the population-based PROFILES registry. Acta Oncol. 2015;54(4):463–9. doi: 10.3109/0284186X.2014.980912. [PubMed: 25417732]
6. Finnerup NB, Attal N, Haroutounian S, McNicol E, Baron R, Dworkin RH, Gilron I, Haanpaa M, Hansson P, Jensen TS, Kamerman PR, Lund K, Moore A, Raja SN, Rice AS, Rowbotham M, Sena E, Siddall P, Smith BH, Wallace M. Pharmacotherapy for neuropathic pain in adults: a systematic review and meta-analysis. Lancet Neurol. 2015;14(2):162–73. doi: 10.1016/S1474-4422(14)70251-0. [PubMed: 25575710]
7. Kaley TJ, Deangelis LM. Therapy of chemotherapy-induced peripheral neuropathy. Br J Haematol. 2009;145(1):3–14. doi: 10.1111/j.1365-2141.2008.07558.x. [PubMed: 19170681]
8. Rowinsky EK, Donehower RC. The clinical pharmacology of paclitaxel (Taxol). Seminars in oncology. 1993;20(4 Suppl 3):16–25. Epub 1993/08/01.

9. Wani MC, Taylor HL, Wall ME, Coggon P, McPhail AT. Plant antitumor agents. VI. The isolation and structure of taxol, a novel antileukemic and antitumor agent from Taxus brevifolia. J Am Chem Soc. 1971;93(9):2325–7. Epub 1971/05/05. [PubMed: 5553076]
10. Rowinsky EK, Cazenave LA, Donehower RC. Taxol: a novel investigational antimicrotubule agent. Journal of the National Cancer Institute. 1990;82(15):1247–59. Epub 1990/08/01. [PubMed: 1973737]
11. Schiff PB, Horwitz SB. Taxol stabilizes microtubules in mouse fibroblast cells. Proc Natl Acad Sci U S A. 1980;77(3):1561–5. Epub 1980/03/01. [PubMed: 6103535]
12. Hamel E, del Campo AA, Lowe MC, Lin CM. Interactions of taxol, microtubule-associated proteins, and guanine nucleotides in tubulin polymerization. The Journal of biological chemistry. 1981;256(22):11887–94. Epub 1981/11/25. [PubMed: 6117556]
13. Schiff PB, Fant J, Horwitz SB. Promotion of microtubule assembly in vitro by taxol. Nature. 1979;277(5698):665–7. Epub 1979/02/22. [PubMed: 423966]
14. Tarr BD, Yalkowsky SH. A new parenteral vehicle for the administration of some poorly water soluble anti-cancer drugs. J Parenter Sci Technol. 1987;41(1):31–3. [PubMed: 3559832]
15. Swindell CS, Krauss NE, Horwitz SB, Ringel I. Biologically active taxol analogues with deleted A-ring side chain substituents and variable C-2' configurations. J Med Chem. 1991;34(3):1176–84. [PubMed: 1672157]
16. Ringel I, Horwitz SB. Studies with RP 56976 (taxotere): a semisynthetic analogue of taxol. Journal of the National Cancer Institute. 1991;83(4):288–91. [PubMed: 1671606]
17. Mathew AE, Mejillano MR, Nath JP, Himes RH, Stella VJ. Synthesis and evaluation of some water-soluble prodrugs and derivatives of taxol with antitumor activity. J Med Chem. 1992;35(1):145–51. [PubMed: 1346275]
18. Lexicomp online, Hudson, Ohio: Lexi-Comp, Inc.; 2013; January 29, 2017.
19. Authier N, Gillet JP, Fialip J, Eschalier A, Coudore F. Description of a short-term Taxol-induced nociceptive neuropathy in rats. Brain Res. 2000;887(2):239–49. [PubMed: 11134612]
20. Lao J, Madani J, Puertolas T, Alvarez M, Hernandez A, Pazo-Cid R, Artal A, Anton Torres A. Liposomal Doxorubicin in the treatment of breast cancer patients: a review. J Drug Deliv. 2013;2013:456409. doi: 10.1155/2013/456409. [PubMed: 23634302]
21. Rahman AM, Yusuf SW, Ewer MS. Anthracycline-induced cardiotoxicity and the cardiac-sparing effect of liposomal formulation. Int J Nanomedicine. 2007;2(4):567–83. [PubMed: 18203425]
22. O'Brien ME, Wigler N, Inbar M, Rosso R, Grischke E, Santoro A, Catane R, Kieback DG, Tomczak P, Ackland SP, Orlandi F, Mellars L, Alland L, Tendler C, Group CBCS. Reduced cardiotoxicity and comparable efficacy in a phase III trial of pegylated liposomal doxorubicin HCl (CAELYX/Doxil) versus conventional doxorubicin for first-line treatment of metastatic breast cancer. Ann Oncol. 2004;15(3):440–9. [PubMed: 14998846]
23. Stone NR, Bicanic T, Salim R, Hope W. Liposomal Amphotericin B (AmBisome((R))): A Review of the Pharmacokinetics, Pharmacodynamics, Clinical Experience and Future Directions. Drugs. 2016;76(4):485–500. doi: 10.1007/s40265-016-0538-7. [PubMed: 26818726]
24. Koudelka S, Turanek J. Liposomal paclitaxel formulations. J Control Release. 2012;163(3):322–34. doi: 10.1016/j.jconrel.2012.09.006. [PubMed: 22989535]
25. Saad M, Garbuzenko OB, Ber E, Chandna P, Khandare JJ, Pozharov VP, Minko T. Receptor targeted polymers, dendrimers, liposomes: which nanocarrier is the most efficient for tumor-specific treatment and imaging? J Control Release. 2008;130(2):107–14. doi: 10.1016/j.jconrel.2008.05.024. [PubMed: 18582982]
26. Yilmaz E, Gold MS. Sensory neuron subpopulation-specific dysregulation of intracellular calcium in a rat model of chemotherapy-induced peripheral neuropathy. Neuroscience. 2015;300:210–8. doi: 10.1016/j.neuroscience.2015.05.019. [PubMed: 25982563]
27. Polomano RC, Mannes AJ, Clark US, Bennett GJ. A painful peripheral neuropathy in the rat produced by the chemotherapeutic drug, paclitaxel. Pain. 2001;94(3):293–304. [PubMed: 11731066]
28. Thangamani D, Edafiogho IO, Masocha W. The anticonvulsant enaminone E139 attenuates paclitaxel-induced neuropathic pain in rodents. ScientificWorldJournal. 2013;2013:240508. doi: 10.1155/2013/240508. [PubMed: 24385872]

29. Aydin TH, Can OD, Demir Ozkay U, Turan N. Effect of subacute agomelatine treatment on painful diabetic neuropathy: involvement of catecholaminergic mechanisms. Fundam Clin Pharmacol. 2016;30(6):549–67. doi: 10.1111/fcp.12224. [PubMed: 27421789]
30. Flatters SJL, Dougherty PM, Colvin LA. Clinical and preclinical perspectives on Chemotherapy-Induced Peripheral Neuropathy (CIPN): a narrative review. Br J Anaesth. 2017;119(4):737–49. doi: 10.1093/bja/aex229. [PubMed: 29121279]
31. Han Y, Smith MT. Pathobiology of cancer chemotherapy-induced peripheral neuropathy (CIPN). Front Pharmacol. 2013;4:156. doi: 10.3389/fphar.2013.00156. [PubMed: 24385965]
32. Seretny M, Currie GL, Sena ES, Ramnarine S, Grant R, MacLeod MR, Colvin LA, Fallon M. Incidence, prevalence, and predictors of chemotherapy-induced peripheral neuropathy: A systematic review and meta-analysis. Pain. 2014;155(12):2461–70. doi: 10.1016/j.pain.2014.09.020. [PubMed: 25261162]
33. Fallon MT. Neuropathic pain in cancer. Br J Anaesth. 2013;111(1):105–11. doi: 10.1093/bja/aet208. [PubMed: 23794652]
34. Sisignano M, Baron R, Scholich K, Geisslinger G. Mechanism-based treatment for chemotherapy-induced peripheral neuropathic pain. Nat Rev Neurol. 2014;10(12):694–707. doi: 10.1038/nrneurol.2014.211. [PubMed: 25366108]
35. Quasthoff S, Hartung HP. Chemotherapy-induced peripheral neuropathy. J Neurol. 2002;249(1):9–17. [PubMed: 11954874]
36. Starobova H, Vetter I. Pathophysiology of Chemotherapy-Induced Peripheral Neuropathy. Front Mol Neurosci. 2017;10:174. doi: 10.3389/fnmol.2017.00174. [PubMed: 28620280]
37. Yamashita Y, Egashira N, Masuguchi K, Ushio S, Kawashiri T, Oishi R. Comparison of Peripheral Neuropathy Induced by Standard and Nanoparticle Albumin–Bound Paclitaxel in Rats. Journal of Pharmacological Sciences. 2011;117(2):116–20. doi: 10.1254/jphs.11062SC. [PubMed: 21897056]
38. Park IH, Sohn JH, Kim SB, Lee KS, Chung JS, Lee SH, Kim TY, Jung KH, Cho EK, Kim YS, Song HS, Seo JH, Ryoo HM, Lee SA, Yoon SY, Kim CS, Kim YT, Kim SY, Jin MR, Ro J. An Open-Label, Randomized, Parallel, Phase III Trial Evaluating the Efficacy and Safety of Polymeric Micelle-Formulated Paclitaxel Compared to Conventional Cremophor EL-Based Paclitaxel for Recurrent or Metastatic HER2-Negative Breast Cancer. Cancer Res Treat. 2017;49(3):569–77. doi: 10.4143/crt.2016.289. [PubMed: 27618821]
39. Paclitaxel liposome for injection [package insert in Chinese]. Nanjing, China Luye Pharma Group2007.
40. Meerum Terwogt JM, ten Bokkel Huinink WW, Schellens JH, Schot M, Mandjes IA, Zurlo MG, Rocchetti M, Rosing H, Koopman FJ, Beijnen JH. Phase I clinical and pharmacokinetic study of PNU166945, a novel water-soluble polymer-conjugated prodrug of paclitaxel. Anticancer Drugs. 2001;12(4):315–23. [PubMed: 11335787]
41. Hamaguchi T, Matsumura Y, Suzuki M, Shimizu K, Goda R, Nakamura I, Nakatomi I, Yokoyama M, Kataoka K, Kakizoe T. NK105, a paclitaxel-incorporating micellar nanoparticle formulation, can extend in vivo antitumour activity and reduce the neurotoxicity of paclitaxel. Br J Cancer. 2005;92(7):1240–6. doi: 10.1038/sj.bjc.6602479. [PubMed: 15785749]
42. Doyle T, Chen Z, Muscoli C, Bryant L, Esposito E, Cuzzocrea S, Dagostino C, Ryerse J, Rausaria S, Kamadulski A, Neumann WL, Salvemini D. Targeting the overproduction of peroxynitrite for the prevention and reversal of paclitaxel-induced neuropathic pain. J Neurosci. 2012;32(18):6149–60. doi: 10.1523/JNEUROSCI.6343-11.2012. [PubMed: 22553021]
43. Masocha W Gene expression profile of sodium channel subunits in the anterior cingulate cortex during experimental paclitaxel-induced neuropathic pain in mice. PeerJ. 2016;4:e2702. doi: 10.7717/peerj.2702. [PubMed: 27896032]
44. Alvarez P, Ferrari LF, Levine JD. Muscle pain in models of chemotherapy-induced and alcohol-induced peripheral neuropathy. Ann Neurol. 2011;70(1):101–9. doi: 10.1002/ana.22382. [PubMed: 21786301]

Highlights

- Liposomal paclitaxel did not lead to neuropathy that was observed for Taxol® group
- Biodisposition data qualified previously developed physiologically-based model
- Liposomal paclitaxel reduced exposure in skin, muscle, brain, spinal cord
- Similar exposure to paclitaxel was observed in skin and muscle tissues

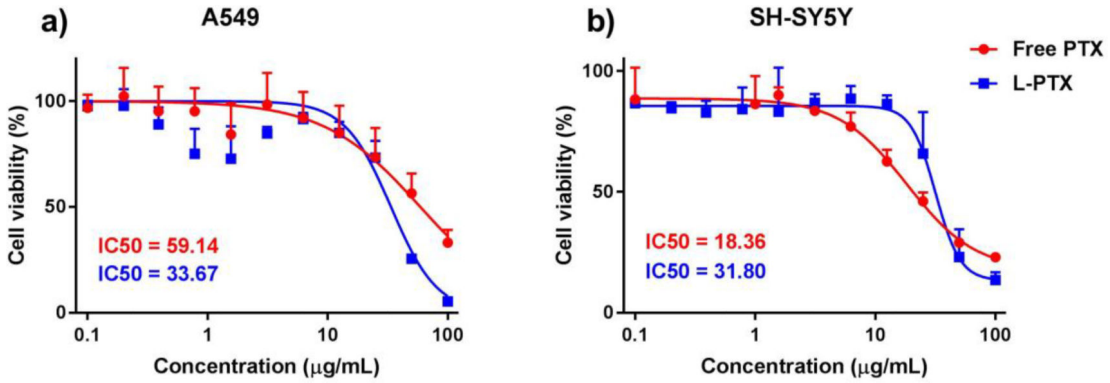

Figure 1.

Cell viability (CellTiter-Fluor™ assay) after incubation with various concentrations of L-PTX formulation and paclitaxel solution for 24 hours **a)** lung cancer cell line A549 and **b)** neuroblastoma cell line SH-SY5Y from 0.1 –100 μg/mL. Data are shown as mean ± SD (n=3). Lines are fitted curves.

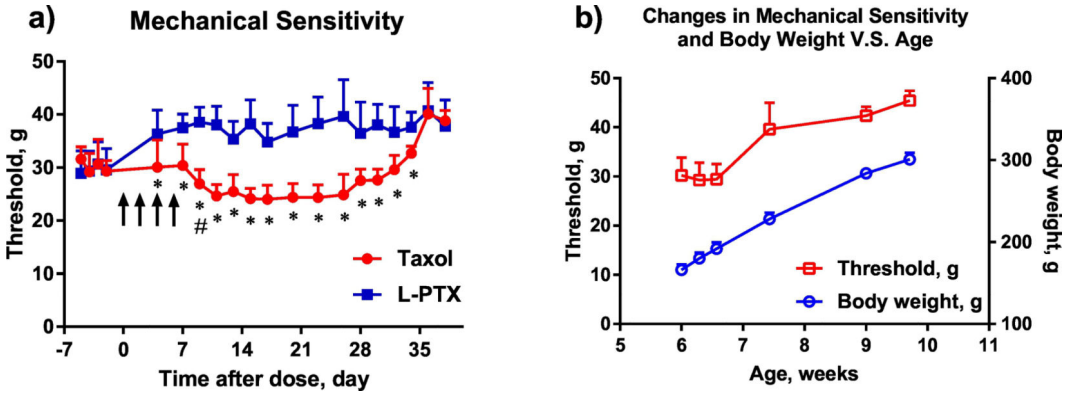

Figure 2.

a) Threshold for withdrawal in response to mechanical stimulation to the plantar surface of hind paw (using Ugo Basile dynamic plantar aesthesiometer) before and after tail vein injection of L-PTX or Taxol® at 2 mg/kg for 4 times (n = 10 each group). Statistically significant difference between treatment groups (* $p < 0.05$), and before and after Taxol® treatment ($^{\#}$ – the first day that the significance ($p < 0.05$) vs. baseline was reached). Arrows indicate days of drug administration. **b)** Changes to the mechanical sensitivity threshold and animal body weight in a group without drug administration. Data are shown as mean ± SD (n=10).

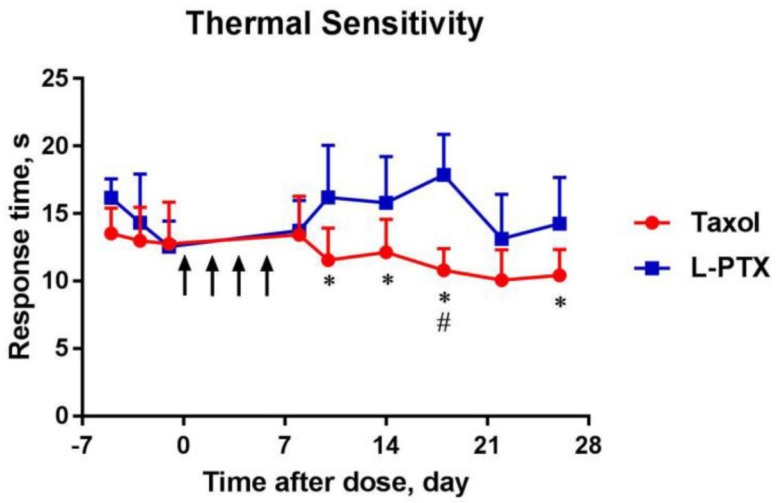

Figure 3.

Response time to thermal stimulation to the plantar surface of hind paw (using Ugo Basile Hargreaves apparatus) before and after injection of L-PTX or Taxol® at 2 mg/kg for 4 times (n = 10 each group). Statistically significant difference between treatment groups (* $p < 0.05$) or before and after Taxol® treatment ($^{\#}$ $p < 0.05$). Arrows indicate days of drug administration. Data are shown in mean ± SD.

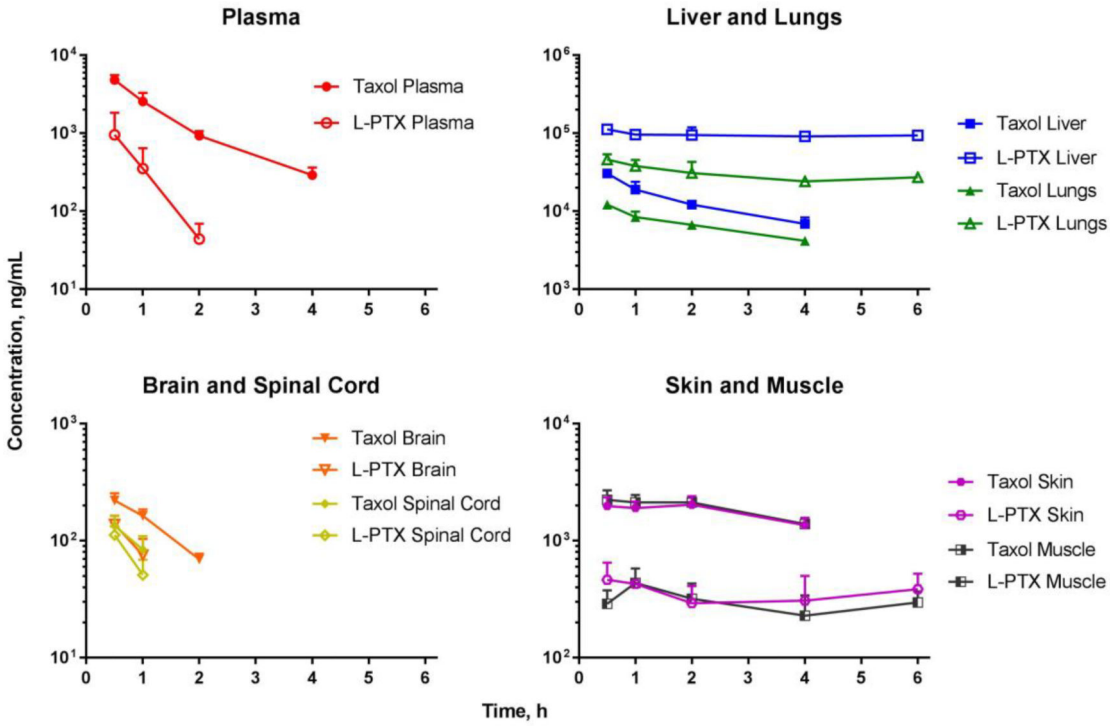

Figure 4.

Exposure to paclitaxel in the plasma, liver, lungs, brain, spinal cord, skin, and muscle, for Taxol® (filled symbols) and L-PTX (open symbols) groups after IV administration (tail vein) at a dose level of 6 mg/kg to rats. Data are presented as mean ± SD (n=3–4).

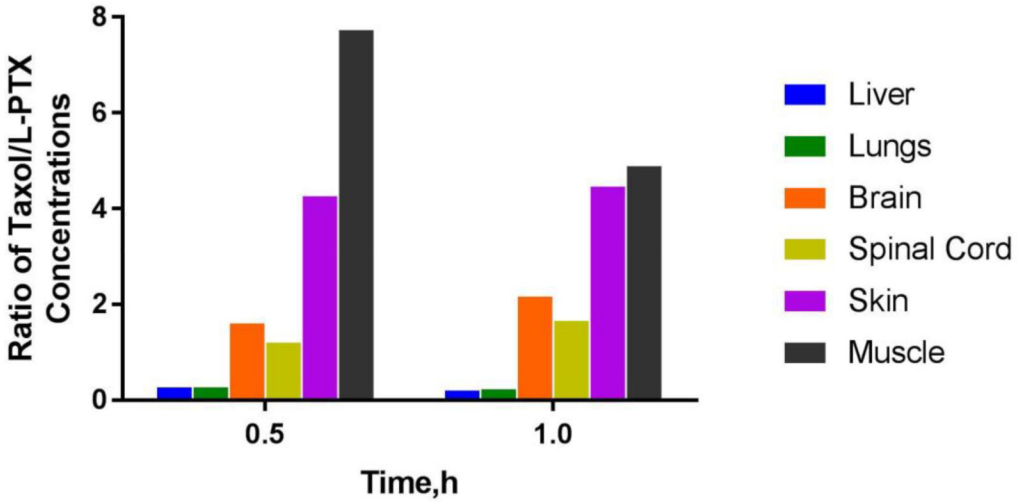

Figure 5.

Ratio of paclitaxel concentrations in the liver, lungs, brain, spinal cord, skin, and muscle at 0.5 and 1 h in rats following IV bolus administration of Taxol® or L-PTX at 6 mg/kg (n=3–4).

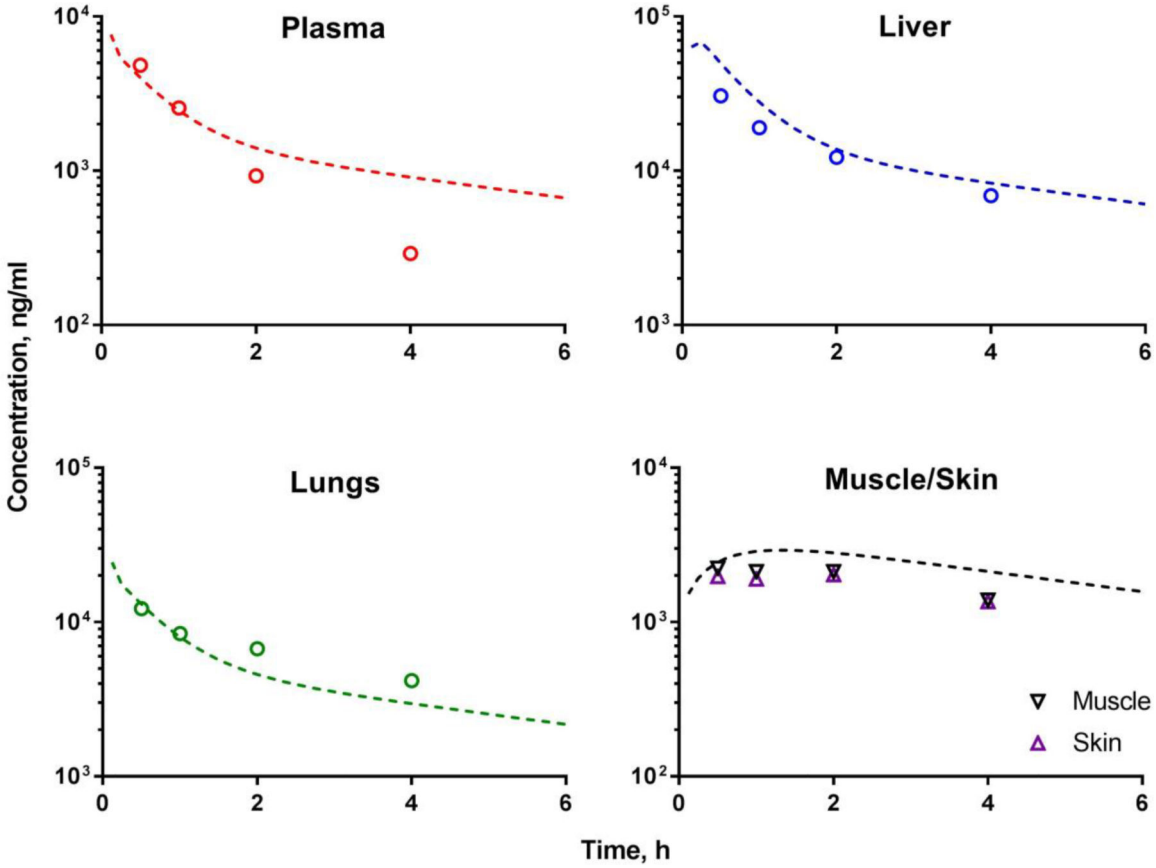

Figure 6.

Observed paclitaxel tissue distribution (open symbols) after IV administration of Taxol® 6 mg/kg overlaid with predictions generated using previously developed physiologically-based pharmacokinetic model (1) (dotted lines) for plasma, liver, lungs, skin, and muscle tissues. In the model, skin and muscle were lumped into a 'remainder' compartment; the simulated line on skin/muscle panel represents a profile for the 'remainder' compartment. Symbols represent experimental mean data obtained in this study (n=3–4).

Table 1.

Plasma pharmacokinetic parameters of paclitaxel after single IV administration of Taxol® and L-PTX formulations to rats (n=4)

PK Parameters	$t_{1/2}$	C_0	AUC_{last}	V_{ss}	CL_T	MRT
	h	ng/mL	ng*h/mL	mL/kg	mL/h/kg	h
Taxol®	1.06	9126	7872	857	721	0.94
L-PTX	0.33	2599	1275	2283	4630	0.46

AUC_{last}, area under the curve to the last measurable concentration; C_0, concentration at time 0 h; CL_T, total body clearance; MRT, mean residence time; $t_{1/2}$, half-life; V_{ss}, volume of distribution at steady state.